Block Spin Ground State and Three-Dimensionality of $(K, Tl)_yFe_{1.6}Se_2$

Chao Cao[1] and Jianhui Dai[1,2]

[1]*Condensed Matter Physics Group, Department of Physics, Hangzhou Normal University, Hangzhou 310036, China*
[2]*Department of Physics, Zhejiang University, Hangzhou 310027, China*

(Received 10 February 2011; published 27 July 2011)

The magnetic properties and electronic structure of $(K, Tl)_yFe_{1.6}Se_2$ is studied using first-principles calculations. The ground state is checkerboard antiferromagnetically coupled blocks of the minimal Fe_4 squares, with a large block-spin moment $\sim 11.2\mu_B$. The magnetic interactions could be modeled with a simple spin model involving both the inter- and intrablock, as well as the nearest-neighbor and next-nearest-neighbor couplings. The calculations also suggest a metallic ground state except for $y = 0.8$ where a band gap ~400–550 meV opens, showing an antiferromagnetic insulator ground state for $(K, Tl)_{0.8}Fe_{1.6}Se_2$. The electronic structure of the metallic $(K, Tl)_yFe_{1.6}Se_2$ is highly three dimensional with unique Fermi surface structure and topology. These features indicate that the Fe-vacancy ordering is crucial to the physical properties of $(K, Tl)_yFe_{2-x}Se_2$.

DOI: 10.1103/PhysRevLett.107.056401 PACS numbers: 71.10.Hf, 71.27.+a, 71.55.−i, 75.20.Hr

Superconductivity (SC) with moderate high transition temperatures [1–6] has been observed in a broad family of the iron-based materials. They are typically represented by the 1111-type LaFeAsO [1], the 122-type $BaFe_2As_2$ [7], the 111-type LiFeAs [8], and the 11-type FeSe [9]. The parent compounds of these materials show a universal striplike (collinear) antiferromagnetic (SDW) order [10,11] except for the 11-type iron chalcogenides where the magnetic order is bi-collinear [12,13]. The magnetic properties are closely related to a common two-dimensional Fe-atom square lattice and the electronic structures are featured by the cylinderlike hole and electron pockets around the Γ and M points, respectively, with relatively weak dispersions alone the c axis. By electron or hole doping the Fermi surfaces evolve smoothly in accordance with the rigid-band shift and the SC instability is enhanced once the magnetic order is suppressed [14].

Recently, a new family of the 122-type FeSe compounds $K_yFe_2Se_2$ [15] and $(Tl, K)_yFe_{2-x}Se_2$ [16,17] have been found to exhibit SC with transition temperatures $T_c \sim 30$ K. Moreover, the iron deficient compound $(Tl, K)_yFe_{2-x}Se_2$ shows two remarkable features: (i) The SC (appears for $x \sim 0.12 - 0.3$, $y \sim 1$) is in proximity to an insulating phase (for relatively larger x, or $y \sim 0.8$) [16–18], and (ii) the Fe vacancies may exhibit some ordered superstructures [16]. Early Mössbauer experiments for $TlFe_{2-x}Se_2$ [19] and recent transmission electron microscopy on $KFe_{2-x}Se_2$ (for $x = 0.4 \sim 0.5$) [20] provide clear evidence for the tetragonal and orthorhombic superstructures in the FeSe layer. Previous first-principles calculations suggested that the Fe-vacancy orthorhombic superstructure could be stabilized with a stripelike (collinear) AFM ground state in $(Tl, K)Fe_{1.5}Se_2$ [21,22]. The insulating behavior with an activation gap ~60 meV in transport observed for $x \sim 0.5$ or around [16] could be attributed to a moderate large short-ranged Fe-3d electron correlation, manifesting a possible Mott insulator driven by kinetic energy reduction due to the ordered Fe vacancies [22]. The Mott transition can be indeed realized by a relatively smaller U_c in a two-orbital model with vacancy orderings [23,24].

So far it is unclear about the precise location of the critical Fe deficiency x_c (for $y = 1$), where the metal-insulator transition takes place. One should notice that in experiments the real Fe content is sample dependent and may deviate from the nominal ones, and possibly (in addition to introduce electrons to the FeSe layer), the role of Tl atoms is to stabilize the Fe-vacancy orderings while the role of alkaline atoms (K, Rb, Cs) is to achieve higher Fe content. Among all the iron deficient compounds, $(K, Tl)_yFe_{1.6}Se_2$ ($x = 0.4$) is of special interest due to its closer proximity to the transition point x_c and the peculiar ordering pattern of the Fe vacancies which can be stabilized in tetragonal crystalline superstructure [16,20]. This is the simplest vacancy superstructure with the highest symmetry since all iron atoms are 3-coordinated, equivalently. Thus, it is especially interesting to understand the electronic and magnetic structures of $(K, Tl)_yFe_{1.6}Se_2$ with the tetragonal Fe-vacancy superstructure.

In this Letter, we performed extensive study on $TlFe_{1.6}Se_2$, using the first-principles simulations. We have also performed calculations on $KFe_{1.6}Se_2$ for the magnetic structure as well as the density of states (DOS), which agrees well with $TlFe_{1.6}Se_2$ results. We found that tuning y only leads to the rigid-band shift for a specific Fe deficiency x. Thus our results are valid for the mixture system $(K, Tl)_yFe_{1.6}Se_2$. In particular, we used the Vienna *ab initio* simulation package (VASP) [25,26], which employs the plane-wave basis set and the projected augmented wave (PAW) method [27]. A body-centered orthorhombic primitive cell [Fig. 1(a)] was used throughout the calculation unless otherwise specified. A 360 eV

energy cutoff and a $4 \times 4 \times 4$ Γ-centered k grid were chosen to ensure the convergence of the total energy to 1 meV/cell. All the geometry were optimized until the forces on each atom smaller than 0.01 eV/Å and the total pressure smaller than 0.5 kB. For the DOS calculations, a much finer k grid of $16 \times 16 \times 16$ and the tetrahedra method were used.

Similar to (K, Tl)$Fe_{1.5}Se_2$, (K, Tl)$_y Fe_{1.6}Se_2$ has three different stacking patterns. Here we focus on the in-plane magnetic structure and consider the *AA* stacking only. As indicated in (K, Tl)$Fe_{1.5}Se_2$, the stacking ordering contributes only a negligible secondary correction to the total energy unless it changes the symmetry of the crystal lattice [22]. We also consider the antiferromagnetic (AFM) interlayer coupling while its magnitude is negligible owing to the large interlayer distances. As a check, we performed test calculations on one of our spin configurations. It turns out that interlayer magnetic coupling contribution is <1 meV/Fe for $TlFe_{1.6}Se_2$.

To begin with, we first study the ground state magnetism by considering eight possible in-plane AFM configurations [Figs. 1(c)–1(j)], as well as the nonmagnetic (NM) and ferro-magnetic (FM) orderings. We list the relaxed geometry parameters as well as their relative energies in TABLE I. The AFM0 configuration could be regarded as the checkerboard AFM; whereas the AFM1 and AFM6 configurations are the bi-collinear and zigzag collinear orderings, respectively. Our calculations suggest a ground state of the AFM2 type, whose configuration energy is 433 meV/cell (or 54 meV/Fe) lower than the second lowest (AFM6) configuration. Because of the symmetry of Fe-vacancies, all Fe sites are equivalent in (K, Tl)$_y Fe_{1.6}Se_2$, forming perfect square Fe blocks [indicated by the blue units in Fig. 1(b)] intercalated by Fe-vacancies. The AFM2 configuration can thus be regarded as checkerboard antiferromagnetically coupled blocks of parallel aligned spins. Furthermore, due to the structure distortion induced by the Fe-vacancies, the magnetic couplings could be classified into two groups: the ones within a square block (intrablock) and the ones across two nearby square blocks (interblock). To model our energetic results, we incorporated a spin model involving both the nearest-neighbor (n.n.) and the next-nearest-neighbor (n.n.n.) couplings:

$$H = \sum_{n,\alpha}(J_1 S_{n,\alpha} S_{n,\alpha+1} + J_1' S_{n,\alpha_\delta} S_{n+\delta,\alpha_\delta}) + \sum_{n,\alpha} J_2 S_{n,\alpha} S_{n,\alpha+2} + \sum_{n,\alpha} J_2'(S_{n,\alpha_\delta} S_{n+\delta,\alpha_\delta+1} + S_{n,\alpha_\delta-1} S_{n+\delta,\alpha_\delta}), \quad (1)$$

where n denotes the block index, δ is short for the nearest-neighboring block-to-block n, α is the site index which

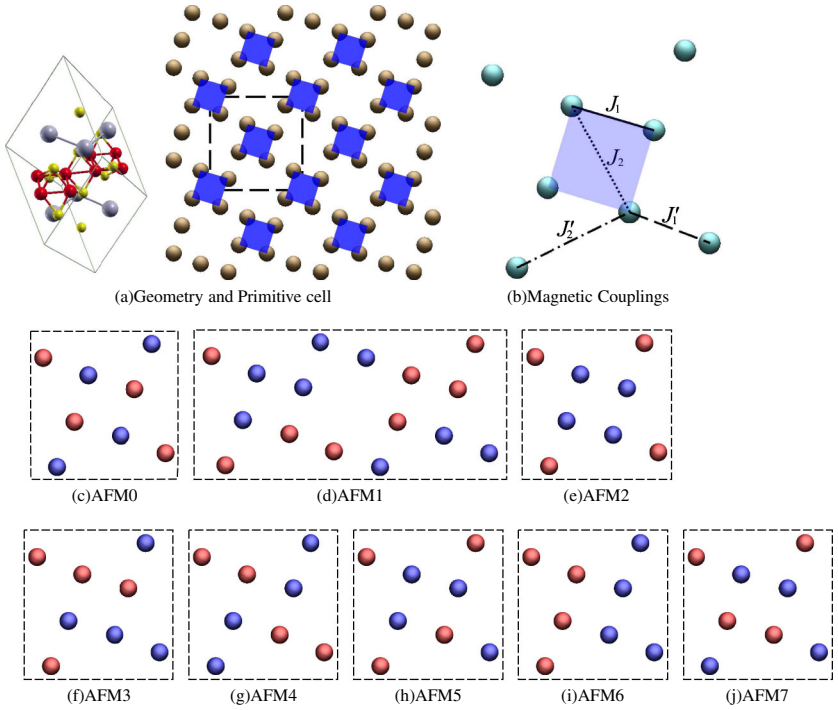

FIG. 1 (color online). 1(a) The geometry and primitive cell from top-view. The shaded (blue) region indicates the fundamental block with the four Fe atoms at the corners. The area encircled by the dashed line for the AFM2 configuration (the ground state) is 74.75 Å^2. The periodic boundary condition for such blocks extended over the whole lattice is imposed. 1(b) The proposed magnetic couplings. (J_1, J_2) and (J_1', J_2') represent the intrablock and interblock (n.n., n.n.n.) couplings, respectively. 1(c)–1(j) are various magnetic configurations. The red/blue atoms indicate the Fe-atoms with positive/negative total magnetic moment, respectively. For the AFM1 configuration, two primitive cells consist a magnetic unit cell. In all figures, we show only the Fe atoms to enhance the visibility.

TABLE I. Lattice constants and magnetic properties of $TlFe_{1.6}Se_2$. The lattice constants are transformed to represent 122 crystal.

	$a(b)$ (Å)	c (Å)	m_{Fe} (μ_B)	E_Δ (meV/Fe)
NM	3.8649(3.8649)	13.1812	0	0
FM	3.7903(3.7904)	14.7087	2.8	−62
AFM0	3.9026(3.9026)	13.6949	2.3	−131
AFM1	3.8494(3.8182)	14.1779	2.7	−183
AFM2	3.8667(3.8668)	14.2420	2.8	**−254**
AFM3	3.8043(3.8517)	14.1884	2.7	−199
AFM4	3.8892(3.8892)	13.9058	2.5	−175
AFM5	3.8882(3.8778)	13.9053	2.6	−180
AFM6	3.7645(3.8440)	14.3045	2.8	−200
AFM7	3.8994(3.8385)	14.0930	2.6	−183

goes from 1 to 4, α_δ selects the site connecting to the nearest-neighboring block δ; J_1 and J_1' (J_2 and J_2') indicate the n.n. (the n.n.n.) couplings of intra- and interblock, respectively. If we further use the approximation that only the S^z component is involved (Ising model with S^z being the same in all configurations at each Fe sites), we could fit the energetics of the 8 AFM configurations using the least squares method to obtain $\tilde{J} = 2JS^2$. The resulting intrablock couplings $\tilde{J}_1$ and $\tilde{J}_2$ are −86 and −9 meV, respectively; while the interblock couplings $\tilde{J}_1'$ and $\tilde{J}_2'$ are −29 and 38 meV, respectively, with fitting correlation $\sigma =$ 97.04%. The AFM interblock n.n.n. interaction $\tilde{J}_2'$ dominates the interblock interactions and both intrablock interactions are FM, thus a block-type checkerboard AFM configuration is favored.

We then examine the electronic structure of $(K, Tl)_yFe_{1.6}Se_2$. We show the band structures of the AFM2 and NM states for $y = 1.0$ in Figs. 2(b) and 2(a), respectively. The band structure of the AFM2 state suggests a metallic nature, with a band gap ∼400 meV for $TlFe_{1.6}Se_2$ (or 550 meV for $KFe_{1.6}Se_2$) for the states 16 meV (or 39 meV) below E_F. Interestingly, the DOS from the top of the band gap to E_F integrates to exactly 0.2 electron per $(K, Tl)_yFe_{1.6}Se_2$ ($y = 1.0$) formula, suggesting that the material would become an insulator if (K, Tl) content is decreased by 20%. As a check, we have further performed calculations for $K_{0.8}Fe_{1.6}Se_2$, assuming two types of K-vacancy orderings [28]. Then a band gap ∼600 meV shows up at E_F for either cases. The result implies that the K vacancies shift the chemical potential but their orderings do not change the band structures.

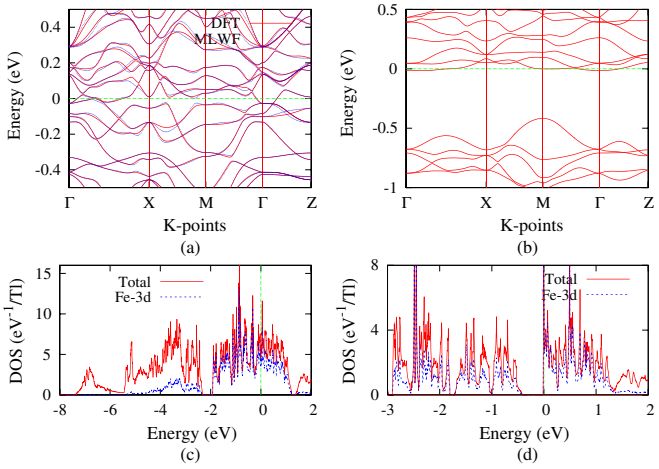

FIG. 2 (color online). Band structure and DOS for $TlFe_{2-x}Se_2$: The left and right panels are for the NM and AFM2 states, respectively. Only up-spin is shown in panels 2(a) and 2(c) since the up- and down-spins are degenerate.

Another interesting feature of the $(K, Tl)_yFe_{1.6}Se_2$ electronic structure is that in the NM state the band energies disperse significantly along k_z axis, manifesting its highly three-dimensional characteristics. This feature is fundamentally different from the KFe_2Se_2 compound [29] and all other iron pnictides. Of course, both the NM and AFM DOS indicate that the Fe-3d orbitals dominate the states near E_F, similar to all iron-based superconductors.

Finally, we reconstruct the Fermi surfaces (Fig. 3) of the metallic $(K, Tl)_yFe_{1.6}Se_2$ ($y = 1.0$) by fitting the band structure using the maximally localized wannier functions (MLWFs) [30,31]. The Fermi surface of both NM and block-spin AFM $(K, Tl)_yFe_{1.6}Se_2$ are highly three- dimensional, although their specific shape is quite different from each other. It is worthwhile to notice that due to the Fe-vacancy superstructure the first Brillouin zone (BZ) is not the same as the one in $(K, Tl)Fe_2Se_2$, and thus the M point in Fig. 3 is not $(\pi/a, \pi/a)$. Nevertheless, the Fermi surface

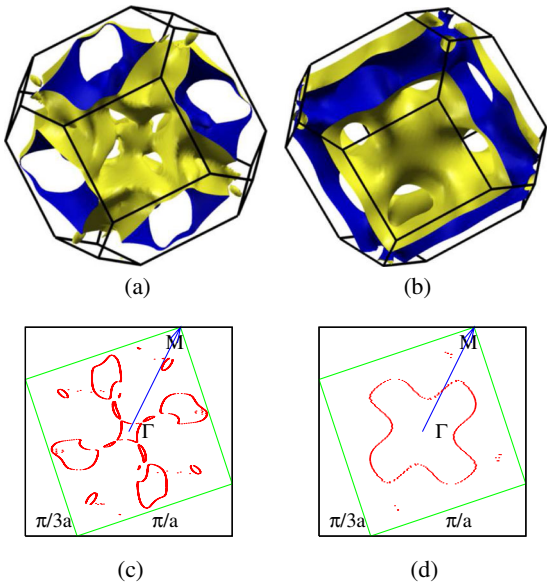

FIG. 3 (color online). Fermi surfaces of $TlFe_{1.6}Se_2$ reconstructed using MLWFs at (a),(c): nonmagnetic (NM) state and (b),(d): block-spin antiferromagnetic state; (c),(d): Cross section of the Fermi surface of $TlFe_{2-x}Se_2$ at $k_z = 0.0$ plane with $x =$ 0.4. Both NM and block-spin AFM Fermi surfaces are 3D-like.

topology of the present $(K, Tl)_yFe_{1.6}Se_2$ compound is quite unique compared to either KFe_2Se_2 [29] or all other iron pnictides. It strongly indicates that the formation of Fe-vacancy superstructures is crucial to the electronic structures of the $(K, Tl)_yFe_{2-x}Se_2$ compounds. Unlike the change in y, the topological change of the Fermi surface across $x \sim 0.4$ indicates that the electronic and magnetic structures for different Fe-vacancy ordered materials cannot be approached by a rigid shift of the chemical potential.

It is worth noting that while the Fe-vacancy ordering is crucial to the block-spin magnetic pattern and the finite gap for $(K, Tl)_{0.8}Fe_{1.6}Se_2$, the strong disorder of the Fe-vacancies may destroy the magnetic ordering leading to the metallic ground state. In the vacancy disordered state, the first Brillouin Zone would remain the same as $(K, Tl)Fe_2Se_2$ and thus the rigid-band model would remain effective. The whole electronic structure in that case could then be approximated with a hole-doped $(K, Tl)_yFe_2Se_2$ [29]. Actually, it has been suggested that randomly distributed Fe-vacancies in the doped antiferromagnetic (or Mott) insulator may lead to a spin-singlet s-wave superconductor [24].

In conclusion, we have performed first-principles calculations on $(K, Tl)_yFe_{1.6}Se_2$. A block-type checkerboard antiferromagnetic ground state was identified and the AFM interblock n.n.n. coupling interaction dominates. Our calculations suggest a metallic ground state for $y = 1$ with a 400–550 meV band gap which appears slightly below the Fermi level and an insulating ground state for $(K, Tl)_{0.8}Fe_{1.6}Se_2$. The experimentally observed insulating behavior may be due to both the 20% (K, Tl) deficiency and the iron vacancy superstructure. Furthermore, the electronic structures of the metallic states show a significant three-dimensional feature with a unique Fermi surface topology, indicating that the formation of Fe-vacancy superstructure is crucial to the physical properties of $(K, Tl)_yFe_{2-x}Se_2$.

The authors would like to thank Q. Si, M. H. Fang, and H. D. Wang for helpful discussions. All calculations were performed at the High Performance Computing Center of Hangzhou Normal University College of Science. This work was supported by the NSFC, the NSF of Zhejiang Province (No.Z6110033), the 973 Project of the MOST and the Fundamental Research Funds for the Central Universities of China (No. 2010QNA3026).

Note added.— Recently, we became aware of a paper by W. Bao *et al.* [32] on the neutron diffraction experiment for $K_{0.8}Fe_{1.6}Se_2$. Our result is in agreement with the reported magnetic ordering pattern.

[1] Y. Kamihara, T. Watanabe, M. Hirano, and H. Hosono, J. Am. Chem. Soc. **130**, 3296 (2008).
[2] X. H. Chen, G. W. T. Wu, R. H. Liu, H. Chen, and D. F. Fang, Nature (London) **453**, 761 (2008).
[3] G. F. Chen, Z. Li, D. Wu, G. Li, W. Z. Hu, J. Dong, P. Zheng, J. L. Luo, and N. L. Wang, Phys. Rev. Lett. **100**, 247002 (2008).
[4] Z. Ren *et al.*, Europhys. Lett. **83**, 17 002 (2008).
[5] H. H. Wen, G. Mu, L. Fang, H. Yang, and X. Zhu, Europhys. Lett. **82**, 17 009 (2008).
[6] C. Wang *et al.*, Europhys. Lett. **83**, 67 006 (2008).
[7] M. Rotter, M. Tegel, and D. Johrendt, Phys. Rev. Lett. **101**, 107006 (2008).
[8] X. Wang, Q. Liu, Y. Lv, W. Gao, L. Yang, R. Yu, F. Li, and C. Jin, Solid State Commun. **148**, 538 (2008).
[9] F. Hsu, Proc. Natl. Acad. Sci. U.S.A. **105**, 14 262 (2008).
[10] C. de la Cruz *et al.*, Nature (London) **453**, 899 (2008).
[11] Y. Qiu *et al.*, Phys. Rev. Lett. **101**, 257002 (2008).
[12] W. Bao *et al.*, Phys. Rev. Lett. **102**, 247001 (2009).
[13] F. Ma, W. Ji, J. Hu, Z.-Y. Lu, and T. Xiang, Phys. Rev. Lett. **102**, 177003 (2009).
[14] J. Paglione and R. Greene, Nature Phys. **6**, 645 (2010).
[15] J. Guo, S. Jin, G. Wang, K. Zhu, M. He, and X. L. Chen, Phys. Rev. B **82**, 180520(R) (2010).
[16] M. Fang, H. Wang, C. Dong, Z. Li, C. Feng, J. Chen, and H. Yuan, Europhys. Lett. **94**, 27 009 (2011).
[17] H. Wang, C. Dong, Z. Li, S. Zhu, Q. Mao, C. Feng, H. Q. Yuan, and M. Fang, Europhys. Lett. **93**, 47 004 (2011).
[18] Z. G. Chen, R. H. Yuan, T. Dong, G. Xu, Y. G. Shi, P. Zheng, J. L. Luo, J. G. Guo, X. L. Chen, and N. L. Wang, Phys. Rev. B **83**, 220507(R) (2011).
[19] L. Haggstrom and A. Seidel, J. Magn. Magn. Mater. **98**, 37 (1991).
[20] Z. Wang, Y. J. Song, H. L. Shi, Z. Wang, Z. Chen, H. F. Tian, G. F. Chen, J. G. Guo, H. X. Yang, and J. Q. Li, Phys. Rev. B **83**, 140505(R) (2011).
[21] X.-W. Yan, M. Gao, Z.-Y. Lu, and T. Xiang, Phys. Rev. Lett. **106**, 087005 (2011).
[22] C. Cao and J. Dai, Phys. Rev. B **83**, 193104 (2011).
[23] R. Yu, J.-X. Zhu, and Q. Si, Phys. Rev. Lett. **106** 186401 (2011).
[24] Y. Zhou, D. Xu, W. Chen, and F. Zhang, Europhys. Lett. **95**, 17 003 (2011).
[25] G. Kresse and J. Hafner, Phys. Rev. B **47**, 558 (1993).
[26] G. Kresse and D. Joubert, Phys. Rev. B **59**, 1758 (1999).
[27] P. E. Blöchl, Phys. Rev. B **50**, 17 953 (1994).
[28] There are two inequivalent K sites, those directly above a Fe_4 block and others. The 2 K-vacancy orderings we assumed refer to the vacancies occupy either of the two sites.
[29] C. Cao and J. Dai, Chin. Phys. Lett. **28**, 057402 (2011).
[30] I. Souza, N. Marzari, and D. Vanderbilt, Phys. Rev. B **65**, 035109 (2001).
[31] A. A. Mostofi, J. R. Yates, Y.-S. Lee, I. Souza, D. Vanderbilt, and N. Marzari, Comput. Phys. Commun. **178**, 685 (2008).
[32] W. Bao, Q. Huang, G. F. Chen, M. A. Green, D. M. Wang, J. B. He, X. Q. Wang, and Y. Qiu, Chin. Phys. Lett. **28**, 086104 (2011).